Robust in-phase synchronization in repressor-based coupled gene oscillators

A B M Shamim Ul Hasan [*], **Supravat Dey** [*],
Hiroyuki Kurata [**], **Abhyudai Singh** [*]

[*] *Department of Electrical and Computer Engineering, University of Delaware, Newark, DE 19716, USA (e-mail: abmsuh@udel.edu,supravat.dey@gmail.com,absingh@udel.edu)*
[**] *Department of Bioscience and Bioinformatics, Kyushu Institute of Technology, 680-4 Kawazu, Iizuka, Fukuoka 820-8502, Japan (e-mail: kurata@bio.kyutech.ac.jp)*

Abstract: Inside living cells, proteins or mRNA can show oscillations even without a periodic driving force. Such genetic oscillations are precise timekeepers for cell-cycle regulations, pattern formation during embryonic development in higher animals, and daily cycle maintenance in most organisms. The synchronization between oscillations in adjacent cells happens via intercellular coupling, which is essential for periodic segmentation formation in vertebrates and other biological processes. While molecular mechanisms of generating sustained oscillations are quite well understood, how do simple intercellular coupling produces robust synchronizations are still poorly understood? To address this question, we investigate two models of coupled gene oscillators - activator-based coupled oscillators (ACO) and repressor-based coupled oscillators (RCO) models. In our study, a single autonomous oscillator (that operates in a single cell) is based on a negative feedback, which is delayed by intracellular dynamics of an intermediate species. For the ACO model (RCO), the repressor protein of one cell activates (represses) the production of another protein in the neighbouring cell after a intercellular time delay. We investigate the coupled models in the presence of intrinsic noise due to the inherent stochasticity of the biochemical reactions. We analyze the collective oscillations from stochastic trajectories in the presence and absence of explicit coupling delay and make careful comparison between two models. Our results show no clear synchronizations in the ACO model when the coupling time delay is zero. However, a non-zero coupling delay can lead to anti-phase synchronizations in ACO. Interestingly, the RCO model shows robust in-phase synchronizations in the presence and absence of the coupling time delay. Our results suggest that the naturally occurring intercellular couplings might be based on repression rather than activation where in-phase synchronization is crucial.

Keywords: Biological oscillations, Coupled oscillators, Interlocked feedback, Stochastic simulation, Noisy gene oscillations

1. INTRODUCTION

The phenomena of oscillations are widely found in living systems. At the cellular level, the gene products such as mRNA/proteins can show sustained oscillations even without any periodic driving force Goldbeter and Berridge (1996); Novák and Tyson (2008); Forger (2017). Such gene oscillations are found in various contexts and across organisms. The popular examples of genetic oscillators are the circadian clock Stokkan et al. (2001); Ray et al. (2020), cell-cycle clock Hara et al. (1980); Pomerening et al. (2003), and segmentation clock Palmeirim et al. (1997); Zinani et al. (2021). The circadian clocks are responsible for maintaining diurnal cycle in most organisms, cell-cycle clocks regulate precise time in cell division, and segmentation clocks dictate accurate rhythmic somite formation during embryonic development in vertebrates.

For the generation of sustained gene oscillations, there are nonlinear regulatory circuits Novák and Tyson (2008).

Depending on contexts, the complexity of such a circuit may vary. However, the basic regulatory motif for many gene oscillators, including the circadian clock, cell-cycle clock, and segmentation clock, is time-delayed negative feedback. The time-delays can arise due to the dynamics of intermediates before the final repression of the clock genes. In eukaryotes, the most contribution of the time-delay comes from the mRNA exportation from the cell nucleus to cytoplasm, importation of cytoplasmic protein to the cell nucleus where transcriptional repression happens, and post-transcriptional modification dynamics. Theoretical models incorporate such delays using explicitly Lewis (2003) or incorporating the dynamics of several intermediates Griffith (1968); Morelli and Jülicher (2007). Such gene regulatory circuits are subject to unavoidable fluctuations due to the inherent stochasticity of biochemical reactions occurring in low molecular abundance Elowitz et al. (2002); Shaffer et al. (2017). Amid such noise, cells produce gene oscillations that are usually remarkably precise Geva-
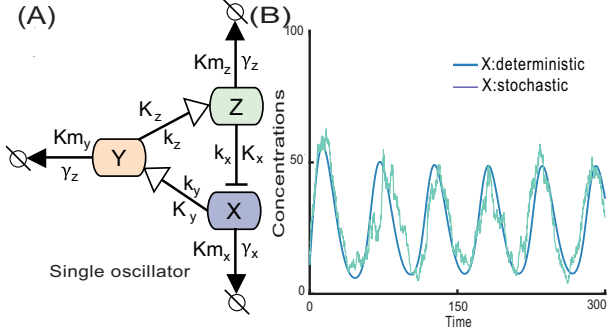
Fig. 1. The schematic of single gene oscillator. (A) A negative feedback loop with three components; where X → Y means 'X activates Y' and X⊣Y means 'X inhibits Y' (B) Trajectories of the deterministic and stochastic simulation of the production of proteins X with $n = 2$. Other parameters: $k_x{=}k_y{=}k_z{=}10$, $\gamma_x{=}\gamma_y{=}\gamma_z{=}8$, $K_x{=}K_y{=}K_z{=}30$, $Km_x{=}Km_y{=}Km_z{=}30$.

Zatorsky et al. (2006); Webb et al. (2016); Keskin et al. (2018). Researchers also successfully engineered synthetic circuits based on delayed repression to generate robust and persistent oscillations in bacteria Elowitz and Leibler (2000); Potvin-Trottier et al. (2016) and mammal cells Tigges et al. (2009).

Although individual cells can act as autonomous oscillators, they must oscillate collectively for proper functions of many biological processes. For example, in the case of segmentation clocks, adjacent cells oscillate in synchrony to produce accurate vertebra formation Lewis (2003); Venzin and Oates (2020). To create such collective oscillations, intercellular coupling between neighbouring cells is essential. Such coupling often involves complex signaling pathways, and its role in synchronization is not well understood Venzin and Oates (2020). Effectively, via intercellular coupling, dynamical changes in molecular concentration of relevant proteins in a cell affect the production of the clock genes in the neighbouring cells. The process of a cell responding to the signal from the neighbours could involve significant amount of time. In essence, the intercellular coupling can activate or repress the production from clock genes in neighbouring cells with some time delay. In this paper, we aim to understand its role by studying two simple models – activator-based coupled oscillators (ACO), and repressor-based coupled oscillators (RCO) models in the presence of coupling delay. The single autonomous oscillator in this study is based on delayed inhibition, where the dynamics of an intermediate species causes the intracellular time delay.

2. MODEL FORMULATION

2.1 Dynamics of single oscillator

The single autonomous gene oscillator consists of three proteins X, Y, and Z (see Fig.1A). The protein X activates Y, and Y activates the expression of Z protein. Finally, protein Z represses the X productions and closes the negative feedback loop. The dynamics of Y and Z causes an effective time delay for the repression. The deterministic dynamics of the concentration of species (denoted as corresponding lower case letters x, y, and z) are given by:

$$\frac{dx}{dt} = k_x f_r(z(t)) - \gamma_x f_d(x(t)), \tag{1a}$$

$$\frac{dy}{dt} = k_y f_a(x(t)) - \gamma_y f_d(y(t)), \tag{1b}$$

$$\frac{dz}{dt} = k_z f_a(y(t)) - \gamma_z f_d(z(t)). \tag{1c}$$

The parameter k_x, k_y, and k_z are the maximum synthesis rates for the protein X, Y and Z, respectively. The maximum degradation rates are denoted by symbols γ_x, γ_y, and γ_z. The functions f_r and f_a are the nonlinear Hill-type functions for the repression and activation Alon (2011); Wilhelmová (1996). These functions are given by

$$f_a(s) = \frac{1}{1 + \left(\frac{K_s}{s}\right)^n} \text{ for } s = x \text{ and } y, \tag{2a}$$

$$f_r(z) = \frac{1}{1 + \left(\frac{z}{K_z}\right)^n}, \tag{2b}$$

where n is the Hill coefficient for the activation and repression, and K_x, K_y and K_z the dissociation constant, representing the values of respective protein concentrations where repression and activation become half of its maximum value. We consider the Michaelis-Menten type degradation, assuming that substrate concentrations are in excess and association equilibria quickly attained. The degradation function f_d for a species S is given by

$$f_d(s) = \frac{s}{Km_s + s} \text{ for } s = x, \ y, \text{ and } z, \tag{3}$$

where the parameter Km_s dissociation constant corresponding to Michaelis-Menten degradation.

In circadian clocks, protein degradation is controlled by phosphorylation, ubiquitination, and proteasomal degradation and thus it is reasonable to assume Michaelis–Menten kinetics Goldbeter (2013); Gonze et al. (2005); Griffith (1968); Purcell et al. (2010); Novák and Tyson (2008). We note that in the limit of linear activation and linear degradation, the model reduced to the well-known Goodwin oscillator, where the repression term is the only source of nonlinearity Goodwin (1965); Griffith (1968). For the latter case, to get sustained oscillations, the Hill coefficient for the repression must be greater than 8 Griffith (1968). As the Goodwin oscillator assumes a minimal regulatory mechanism for generating sustained oscillations, it is beneficial for mathematical insights Griffith (1968); Dey and Singh (2020). However, such a high Hill coefficient value is often considered biologically unrealistic Gonze and Abou-Jaoudé (2013). With other nonlinearities coming from activation and Michaelis-Menten, in our model, one can get sustained oscillations even with the Hill coefficient $n = 2$. Here, the typical trajectories of species X for $n = 2$ is shown in Fig. 1B.

Table 1. Definition of the kinetic parameters

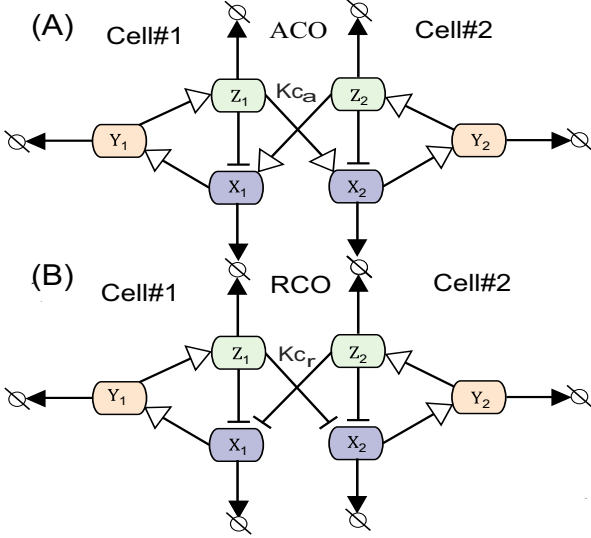| Kinetic parameter	Description
k_x, k_y, k_z	synthesis rate const.
$\gamma_x, \gamma_y, \gamma_z$	protease (enzyme) rate const.
K_x, K_y, K_z	dissociation const. for activation/repression
Km_x, Km_y, Km_z	dissociation const. for Michaelis-Menten
Kc_a, Kc_r	coupling dissociation const.
n	Hill coefficient
τ	coupling time-delay

Fig. 2. The Schematic diagrams of the models of coupled oscillators. A single oscillator operates in a single cell. Both cells are identical and the coupling acts symmetrically between them. (A) The ACO model: the protein Z in one cell activates the production of protein X in the other cell. (B) The ACO model: the protein Z in one cell represses the production of protein X in the other cell.

2.2 Dynamics of coupled oscillators

The oscillator in each cells are coupled to its adjacent cell via signaling pathway. Such coupling are essential for synchronization between oscillations in neighboring cells. The signaling pathways often complex that involves several molecular species undergoing many biochemical reactions. Such complexity makes theoretical studies of synchronizations challenging Venzin and Oates (2020).

Here we study two different models of two coupled oscillators with opposite coupling mechanisms, schematically shown in Fig. 2. In our models, we do not have additional signaling species for intercellular coupling. The protein Z itself acts as a signaling molecule and affects the production of protein X in the other cell with some time delay τ. We consider two coupling mechanisms: activator-based coupled oscillators (ACO) and repressor-based coupled oscillators (RCO). More specifically, in ACO, Z in a cell activates the production of X in the other cell. Whereas in RCO, Z represses the production of X in the other cell. In our study, we assume both oscillators are identical and the coupling acts symmetrically between two oscillators. The coupling directly affects the production of X, whose deterministic dynamics for a cell $i = \{1, 2\}$ is given by

$$\frac{dx_i}{dt} = k_x f_{ac}(z_i(t), z_j(t-\tau)) - \gamma_x f_d(x_i(t)) : \text{for ACO}, \quad (4a)$$

$$\frac{dx_i}{dt} = k_x f_{rc}(z_i(t), z_j(t-\tau)) - \gamma_x f_d(x_i(t)) : \text{for RCO}, \quad (4b)$$

where j is the neighbour of i. The coupling functions for ACO f_{ac} and for RCO f_{rc} are

$$f_{ac}(z_i(t), z_j(t-\tau)) = f_r(z_i(t)) f_a(z_j(t-\tau))$$
$$= \frac{1}{1 + (\frac{z_i(t)}{K_z})^n} \frac{1}{1 + (\frac{Kc_a}{z_j(t-\tau)})^n}, \quad (5a)$$

$$f_{rc}(z_i(t), z_j(t-\tau)) = f_r(z_i(t)) f_r(z_j(t-\tau))$$
$$= \frac{1}{1 + (\frac{z_i(t)}{K_z})^n} \frac{1}{1 + (\frac{z_j(t-\tau)}{Kc_r})^n}, \quad (5b)$$

where Kc_a and Kc_r are the corresponding coupling dissociation constants. We note that for ACO, in the limit of $Kc_a \to 0$, both oscillators become uncoupled, whereas for RCO the uncoupled limit is $Kc_r \to \infty$. The dynamics of Y and Z proteins are not directly affected by the coupling and are given by

$$\frac{dy_i}{dt} = k_y f_a(x_i(t)) - \gamma_y f_d(y_i(t)), \quad (6a)$$

$$\frac{dz_i}{dt} = k_z f_a(y_i(t)) - \gamma_z f_d(z_i(t)). \quad (6b)$$

The gene expression is noisy as the biochemical reactions are inherently stochastic, and such noise becomes crucial when the molecular species inside cells present in low abundances. Thus, we study the above coupled systems in the presence of such intrinsic noise. As our coupling explicitly depends on the time-delay, we can not use the traditional stochastic simulations algorithm Gillespie (1977). Here, we employ the time-delay stochastic simulation algorithm as proposed in Barrio et al. (2006).

3. RESULTS

3.1 Collective oscillations without intercellular time delay

First, we study collective oscillations in the absence of intercellular coupling time delay ($\tau = 0$) by varying the coupling dissociation constant which is a measure of coupling strength. Then, we study the effect of the coupling time delay. As the ACO and RCO models work very differently, comparing their the collective oscillations in these two models can be tricky. We do the following mathematical comparison between the ACO and RCO.

Mathematical comparison between ACO and RCO: We keep parameters for the single oscillators in both the ACO and RCO models the same. For comparison, we conserve the amplitude or period of the oscillations for both these models and then study the synchronization. To conserve the amplitude or period, we only vary the coupling dissociation constant. This is very much in the spirit of the mathematically controlled comparison Hasan and Kurata (2017); Hasan et al. (2019); Hasan and Kurata (2016); Alves and Savageau (2000).

Table 2. Parameters for the ACO and RCO models to conserve the expression levels.

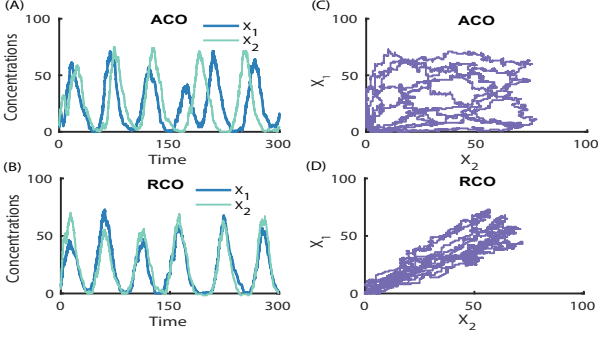| Each network	ACO	RCO
	$k_x=k_y=k_z=10$	$k_x=k_y=k_z=10$
Corresponding	$\gamma_x=\gamma_y=\gamma_z=8$	$\gamma_x=\gamma_y=\gamma_z=8$
parameters	$K_x=K_y=30$	$K_x=K_y=30$
	$K_z=30$	$K_z=30$
	$Km_x=Km_y=30$	$Km_x=Km_y=30$
	$Km_z=30$	$Km_z=30$
	$Kc_a=1.1$	$Kc_r=30$
	$n=3$	$n=3$
	$\tau=0$	$\tau=0$

Fig. 3. Stochastic simulation results for the ACO and RCO models at conserved expression levels. Trajectories of concentration of protein X for cells 1 and 2 for the ACO and RCO models are plotted in (A) and (B), respectively. (C) and (D) are the scatter plots of X_1 and X_2 corresponding to (A) and (B). For the RCO, the trajectories of both cells follow each other, suggesting a strong in-phase synchronization. For the ACO, the trajectories of both cells seem random, suggesting no clear phase synchronization.

A. Coupled oscillators with conserved expression levels.
To conserve the expression levels of protein X in the ACO and RCO models, we use the parameter set presented in Table. 2. We only vary the value of the coupling dissociation constants, while the values of the other kinetic parameters within each model and between the competitive models are the same. The results are presented in Fig. 3. The RCO model shows robust in-phase synchronization. Whereas, the ACO model does not show any clear phase synchronizations – cell-1 and cell-2 seem to oscillate randomly.

Table 3. Parameters for the ACO and RCO models to conserve the expression period.

Each network	ACO	RCO
	$k_x=k_y=k_z=10$	$k_x=k_y=k_z=10$
Corresponding	$\gamma_x=\gamma_y=\gamma_z=8$	$\gamma_x=\gamma_y=\gamma_z=8$
parameters	$K_x=K_y=13.55$	$K_x=K_y=13.55$
	$K_z=13.55$	$K_z=13.55$
	$Km_x=Km_y=13.55$	$Km_x=Km_y=13.55$
	$Km_z=13.55$	$Km_z=13.55$
	$Kc_a=1.1$	$Kc_r=30$
	$n=3$	$n=3$
	$\tau=0$	$\tau=0$

B. Coupled oscillators with conserved period. Is the collective oscillation observed in the conserved expression comparison also holds across other parameters? Here, we make another comparison by keeping the period of the oscillations in both the model the same. The parameters for this case are presented in Table. 3. We only vary the value of the coupling dissociation constants, while the values of the other kinetic parameters within each model and between the competitive models are the same. The results are presented in Fig. 4. As in the conserved expression comparison case, we find robust in-phase synchronization for the RCO, while the ACO model shows no clear phase synchronizations.

We also run several stochastic simulations by perturbing parameters presented in Table 2 and Table 3. We find
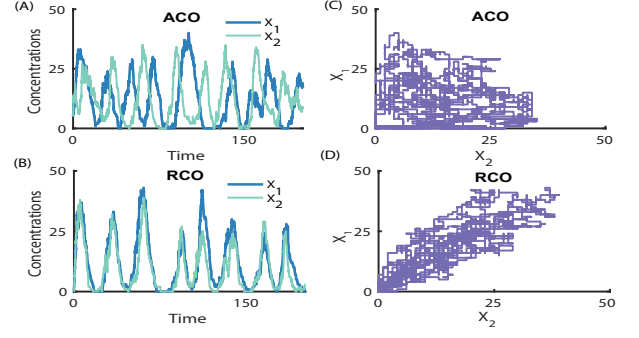

Fig. 4. Stochastic simulation results for the ACO and RCO models at conserved period. Trajectories of concentration of protein X for cells 1 and 2 for the ACO and RCO models are plotted in (A) and (B), respectively. (C) and (D) are the scatter plots of X_1 and X_2 corresponding to (A) and (B). For the RCO, the trajectories of protein X for both cells show strong in-phase synchronization. For the ACO, the trajectories of both cells seem random.

the robust in-phase synchronization for the RCO across parameters. Again, no clear phase synchronization is observed in the ACO model.

3.2 Effect of intercellular time delay

Now, we turn our focus on the effect of the intercellular coupling time delay. Time delay can have an interesting effects on the coupled oscillations Kim et al. (2010); Joshi et al. (2020); Rashid and Kurata (2020); Amdaoud et al. (2007). It also plays a critical role in synchronization between the coupled feedback oscillators Smolen et al. (2001). For example, it can lead to alternative in-phase synchronization and anti-phase as the delay time is varied Jörg et al. (2018); Giordano et al. (2019); Dey et al. (2020). Here, we quantify the collective oscillation by the Pearson correlation coefficient in the presence and absence of coupling delay time τ. If $X_1(t)$ and $X_2(t)$ are the stochastic variables representing the concentration protein X in cell 1 and 2 at time t, respectively, then the Pearson correlation, R between them is given by,

$$R = \frac{\langle X_1 X_2 \rangle - \langle X_1 \rangle \langle X_2 \rangle}{\sqrt{(\langle X_1^2 \rangle - \langle X_1 \rangle^2)(\langle X_2^2 \rangle - \langle X_2 \rangle^2)}}, \qquad (7)$$

where the angular bracket $\langle \cdot \rangle$ denotes the average over time and ensembles. The value of correlation R is 1 if protein X in both cells oscillate in perfect in-phase, -1 if both cells oscillate in perfect anti-phase, 0 if both cells oscillate randomly. We measure the correlation coefficient R, for coupling delay $\tau = 0$ and $\tau = 12$. The period of the oscillations is 24 when $\tau = 0$. For a given τ, we compute R for different values of coupling dissociation constant Kc_a or Kc_r. Each R value is computed averaging over hundreds of long trajectories with time window 8000.

In Fig. 5(A), we plot R as a function of Kc_a and Kc_r for the ACO and RCO model. For $\tau = 0$, R remains close to zero throughout for the ACO, whereas R becomes close to 1 for large values of Kc_r, showing in-phase synchronizations in the RCO and no synchronization the in ACO model. This consistent with the observation discussed in
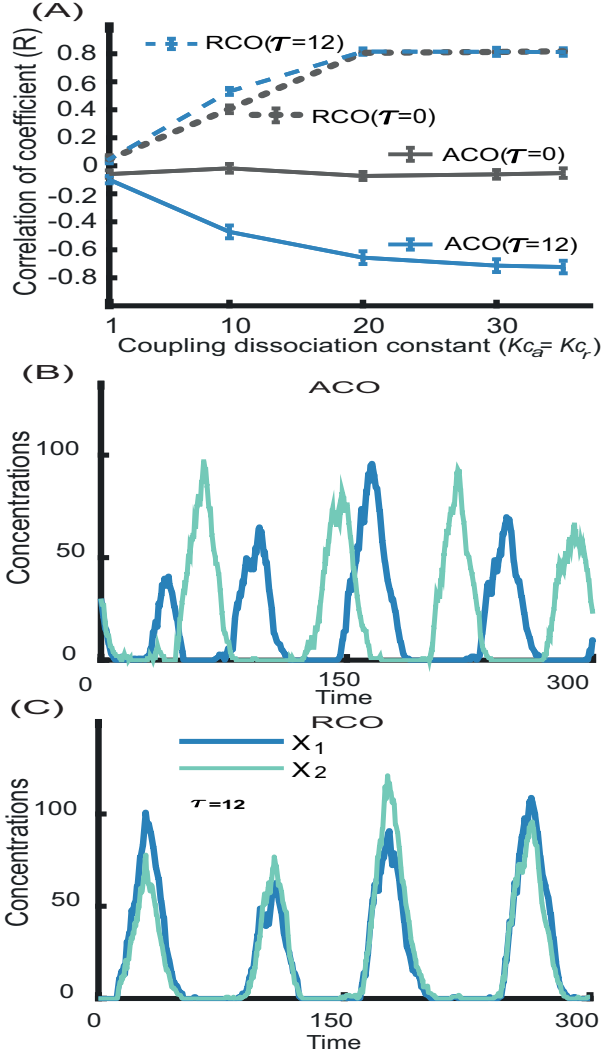
Fig. 5. Effect of coupling time-delay. (A) The correlation R is plotted for $\tau = 0$ and $\tau = 12$ as a functions the coupling dissociation constant. For the RCO, R approaches to 0.8 irrespective of the value of τ, showing strong in-phase synchronizations. While for the ACO, the synchronization behavior depends on the value of τ. When $\tau = 0$, two cells oscillates randomly results $R \approx 0$. For $\tau = 0$, $R \approx -0.8$ for large Kc_a, suggesting an anti-phase synchronization. (B) and (C) The stochastic trajectories for the ACO and RCO for $\tau = 12$ for $Kc_r = Kc_a = 30$. Other parameters are shown Table 3.

the above section. The RCO continues to show in-phase synchronization in the presence of time delay. Interestingly, for a non-zero τ, the value of R becomes close to -1 for large dissociation constant for the ACO, suggesting the development of anti-phase synchronization in the presence of intercellular time delay. The in-phase synchronization in the RCO and anti-phase synchronization in the ACO for a finite τ can also be clearly seen from the stochastic trajectory plots (Fig. 5(B) and (C)).

4. CONCLUSION

Synchronizations of genetic oscillators are crucial for many biological processes, including precise vertebra formation during embryonic development Lewis (2003); Venzin and Oates (2020). Amid inherent stochastic fluctuations due to biochemical reactions, how do the intercellular coupling leading to robust synchronizations is poorly understood? To understand the role of intercellular coupling, we have developed two models for coupling, namely the ACO (activator-based coupled gene oscillator) and RCO (repressor-based coupled gene oscillators). The impacts of signaling molecules are effectively incorporated via the usual Hill functions. We have included an effective coupling delay due to the dynamics of signaling molecules. The single autonomous oscillator in our study is based on delayed inhibition where the dynamics of intermediate species cause the delay.

We have solved our stochastic systems of coupled oscillators in the presence and absence of delay using the algorithm as proposed in Barrio et al. (2006). We have found that the RCO shows robust in the presence and absence of time delay. Interestingly, in the ACO, we have not found a clear synchronization without coupling delay. However, in the presence of coupling delay, the ACO can lead to anti-phase synchronization. Our results suggest that the naturally occurring intercellular couplings might be based on repression rather than activation, where in-phase synchronization is crucial.

REFERENCES

Alon, U. (2011). *An Introduction to Systems Biology: Design Principles of Biological Circuits.* Chapman and Hall/CRC.

Alves, R. and Savageau, M.A. (2000). Extending the method of mathematically controlled comparison to include numerical comparisons. *Bioinformatics*, 16, 786–798.

Amdaoud, M., Vallade, M., Weiss-Schaber, C., and Mihalcescu, I. (2007). Cyanobacterial clock, a stable phase oscillator with negligible intercellular coupling. *Proceedings of the National Academy of Sciences*, 104, 7051–7056.

Barrio, M., Burrage, K., Leier, A., and Tian, T. (2006). Oscillatory regulation of hes1: discrete stochastic delay modelling and simulation. *PLoS Comput Biol*, 2, e117.

Dey, S. and Singh, A. (2020). Genomic decoy sites enhance the oscillatory regime of a biomolecular clock. In *2020 American Control Conference (ACC)*, 5002–5007.

Dey, S., Tracey, L., and Singh, A. (2020). Role of intercellular coupling and delay on the synchronization of genetic oscillators. *bioRxiv:2020.09.29.318717*.

Elowitz, M. and Leibler, S. (2000). A synthetic oscillatory netwrok of transcriptional regulators. *Nature*, 403, 335–338.

Elowitz, M.B., Levine, A.J., Siggia, E.D., and Swain, P.S. (2002). Stochastic gene expression in a single cell. *Science*, 297, 1183–1186.

Forger, D.B. (2017). *Biological Clocks, Rhythms, and Oscillations: The Theory of Biological Timekeeping.* MIT Press, Cambridge (MA).

Geva-Zatorsky, N., Rosenfeld, N., Itzkovitz, S., Milo, R., Sigal, A., Dekel, E., Yarnitzky, T., Liron, Y., Polak, P., Lahav, G., and Alon, U. (2006). Oscillations and variability in the p53 system. *Molecular Systems Biology*, 2, 2006.0033.

Gillespie, D.T. (1977). Exact stochastic simulation of coupled chemical reactions. *The journal of physical chemistry*, 81, 2340–2361.

Giordano, G., Singh, A., and Blanchini, F. (2019). Analysis of coupled genetic oscillators with delayed positive feedback interconnections. In *2019 18th European Control Conference (ECC)*, 674–679.

Goldbeter, A. (2013). Oscillatory enzyme reactions and michaelis–menten kinetics. *FEBS Letters*, 587(17), 2778–2784.

Goldbeter, A. and Berridge, M.J. (1996). *Biochemical Oscillations and Cellular Rhythms: The Molecular Bases of Periodic and Chaotic Behaviour*. Cambridge University Press.

Gonze, D. and Abou-Jaoudé, W. (2013). The goodwin model: Behind the hill function. *PLOS ONE*, 8, 1–15.

Gonze, D., Bernard, S., Waltermann, C., Kramer, A., and Herzel, H. (2005). Spontaneous synchronization of coupled circadian oscillators. *Biophysical journal*, 89, 120–129.

Goodwin, B.C. (1965). Oscillatory behavior in enzymatic control processes. *Advances in enzyme regulation*, 3, 425–437.

Griffith, J. (1968). Mathematics of cellular control processes i. negative feedback to one gene. *Journal of theoretical biology*, 20, 202–208.

Hara, K., Tydeman, P., and Kirschner, M. (1980). A cytoplasmic clock with the same period as the division cycle in xenopus eggs. *Proceedings of the National Academy of Sciences*, 77, 462–466.

Hasan, A.S.U. and Kurata, H. (2016). Competitive memory functions in gene regulatory network. *JIP*, 2, 1–3.

Hasan, A.S.U. and Kurata, H. (2017). Mathematical comparison of memory functions between mutual activation and repression networks in a stochastic environment. *Journal of Theoretical Biology*, 427, 28–40.

Hasan, A.S.U., Kurata, H., and Pechmann, S. (2019). Improvement of the memory function of a mutual repression network in a stochastic environment by negative autoregulation. *BMC bioinformatics*, 20, 1–14.

Jörg, D.J., Morelli, L.G., and Jülicher, F. (2018). Chemical event chain model of coupled genetic oscillators. *Phys. Rev. E*, 97, 032409.

Joshi, Y.J., Jawale, Y.K., and Athale, C.A. (2020). Modeling the tunability of the dual-feedback genetic oscillator. *Physical Review E*, 101, 012417.

Keskin, S., Devakanmalai, G.S., Kwon, S.B., Vu, H., Soltani, M., Singh, A., Ay, A., and Ozbudak, E.M. (2018). Noise in the vertebrate segmentation clock is boosted by time-delays but tamed by notch signaling. *Cell Reports*, 23, 2175–2185.

Kim, J.R., Shin, D., Jung, S.H., Heslop-Harrison, P., and Cho, K.H. (2010). A design principle underlying the synchronization of oscillations in cellular systems. *Journal of cell science*, 123, 537–543.

Lewis, J. (2003). Autoinhibition with transcriptional delay: a simple mechanism for the zebrafish somitogenesis oscillator. *Current Biology*, 13, 1398–1408.

Morelli, L.G. and Jülicher, F. (2007). Precision of genetic oscillators and clocks. *Phys. Rev. Lett.*, 98, 228101.

Novák, B. and Tyson, J.J. (2008). Design principles of biochemical oscillators. *Nature reviews Molecular cell biology*, 9, 981–991.

Palmeirim, I., Henrique, D., Ish-Horowicz, D., and Pourquié, O. (1997). Avian hairy gene expression identifies a molecular clock linked to vertebrate segmentation and somitogenesis. *Cell*, 91, 639–648.

Pomerening, J.R., Sontag, E.D., and Ferrell, J.E. (2003). Building a cell cycle oscillator: hysteresis and bistability in the activation of cdc2. *Nature Cell Biology*, 5, 346–351.

Potvin-Trottier, L., Lord, N.D., Vinnicombe, G., and Paulsson, J. (2016). Synchronous long-term oscillations in a synthetic gene circuit. *Nature*, 538, 514–517.

Purcell, O., Savery, N.J., Grierson, C.S., and Di Bernardo, M. (2010). A comparative analysis of synthetic genetic oscillators. *Journal of The Royal Society Interface*, 7, 1503–1524.

Rashid, M.M. and Kurata, H. (2020). Coupling protocol of interlocked feedback oscillators in circadian clocks. *Journal of the Royal Society Interface*, 17, 20200287.

Ray, S., Valekunja, U.K., Stangherlin, A., Howell, S.A., Snijders, A.P., Damodaran, G., and Reddy, A.B. (2020). Circadian rhythms in the absence of the clock gene bmal1. *Science*, 367, 800–806.

Shaffer, S.M., Dunagin, M.C., Torborg, S.R., Torre, E.A., Emert, B., Krepler, C., Beqiri, M., Sproesser, K., Brafford, P.A., Xiao, M., Eggan, E., Anastopoulos, I.N., Vargas-Garcia, C.A., Singh, A., Nathanson, K.L., Herlyn, M., and Raj, A. (2017). Rare cell variability and drug-induced reprogramming as a mode of cancer drug resistance. *Nature*, 546, 431–435.

Smolen, P., Baxter, D.A., and Byrne, J.H. (2001). Modeling circadian oscillations with interlocking positive and negative feedback loops. *Journal of Neuroscience*, 21, 6644–6656.

Stokkan, K.A., Yamazaki, S., Tei, H., Sakaki, Y., and Menaker, M. (2001). Entrainment of the circadian clock in the liver by feeding. *Science*, 291, 490–493.

Tigges, M., Marquez-Lago, T.T., Stelling, J., and Fussenegger, M. (2009). A tunable synthetic mammalian oscillator. *Nature*, 457, 309–312.

Venzin, O.F. and Oates, A.C. (2020). What are you synching about? emerging complexity of notch signaling in the segmentation clock. *Developmental Biology*, 460, 40–54.

Webb, A.B., Lengyel, I.M., Jörg, D.J., Valentin, G., Jülicher, F., Morelli, L.G., and Oates, A.C. (2016). Persistence, period and precision of autonomous cellular oscillators from the zebrafish segmentation clock. *eLife*, 5, e08438.

Wilhelmová, N. (1996). Cornish-bowden, a.: fundamentals of enzyme kinetics. *Biologia Plantarum*, 38, 430–430.

Zinani, O.Q.H., Keseroğlu, K., Ay, A., and Özbudak, E.M. (2021). Pairing of segmentation clock genes drives robust pattern formation. *Nature*, 589, 431–436.